Scientia Iranica F (2021) 28(3), 1908–1916

Sharif University of Technology
Scientia Iranica
Transactions F: Nanotechnology
http://scientiairanica.sharif.edu

Preparation and investigation of optical properties and photocatalytic activity of SnO_2/GO thin films

A.H.A. Jalaukhan[a], B. Ghanbari Shohany[b,*], and R. Etefagh[b]

a. *College of Education for Pure Sciences, University of Kerbala, Iraq.*
b. *Borhan Nano Scale Company, Mashhad, Iran.*

Received 29 August 2019; received in revised form 17 November 2020; accepted 17 May 2021

KEYWORDS
SnO_2/GO;
Spin coating method;
Optical properties;
Photocatalytic activity.

Abstract. In this study, tin oxide-pure (SnO_2) and tin oxide/Graphene Oxide (SnO_2/GO) thin films with different concentrations of GO (0, 1, 2, 3, and 4 g/ml) were synthesized using spin coating method. The synthesized thin films were used to study the structural, morphological, chemical, optical, and photocatalytic degradation of Methyl Orange (MO) under UV light irradiation using X-Ray Diffraction (XRD) spectroscopy, Field Emission Scanning Electron Microscopy (FESEM), Raman spectroscopy, and Ultraviolet-Visible (UV-Vis) spectroscopy, respectively. The XRD results of GO showed that the peak was very sharp with high intensity, which was indicative of the quite good crystallinity of the GO structure. The band gap value of SnO_2/GO thin films increased followed by increase in the GO concentration. Under UV light irradiation, the photocatalytic activity of the synthesized samples was measured using MO dye. The obtained results also indicated that adding GO concentration would increase the photocatalytic activity of the SnO_2 thin film.

1. Introduction

Semiconductors with the wide band gap ($E_g > 2.8$ eV) such as indium oxide, tin oxide (SnO_2), zinc oxide, and cadmium oxide have received considerable attention in recent years. These materials are characterized by a high intrinsic density of free charge carriers due to the deviation from the elemental proportion [1–4]. This deviation results from lack of oxygen in the crystalline lattice of these materials. In fact, while adding impurities, the free-charge density would be higher than the intrinsic density (close to the free carrier density of the metal). The electrical conductivity of these materials can be reduced through the impurity injection process, thus reaching the electrical conductivity of the conductors. These materials have been widely applied in technology and industry, e.g., in optoelectronic components (as transparent electrodes), automotive industries, airplanes (as transparent thermal elements), photovoltaic solar cell, and photo detectors (as antistatic coatings) [5–10].

SnO_2 is one of the important wide band gap semiconductors in technology used for a variety of applications in materials science and engineering. SnO_2 thin films are mainly known as transparent conductors whose electrical conductivity after doping them with donor atoms is quite large, i.e., in the order of 10^5 S.cm^{-1} [11–16]. In addition to SnO_2 high optical transparency in the visible region, it has been widely employed due to its mechanical stability, resistance to

*. *Corresponding author.*
E-mail address: bo.gh@mail.um.ac.ir (B. Ghanbari Shohany)

doi: 10.24200/sci.2021.54336.3706

chemical corrosion, and low cost of pristine materials. This semiconductor material is characterized by an energy band gap ranging from 3.7 to 4.2 eV as well as a quadrilateral structure [17–19]. The first report on the preparation of SnO_2 transparent semiconductor layers in 2004 was attributed to the OGALE research group. The above-mentioned layers are characterized by a crystalline structure whose optical transparency in the visible region and carrier density are about 60% and 10^{18} cm^{-3} [20], respectively. In recent years, with the growth of research interests in the transparent magnetic semiconductors field, researchers have studied the construction of transparent semiconducting magnetic SnO_2 with considerable impurities [21–23].

Another application of SnO_2 is the photocatalytic degradation of organic pollutants in the water and air, which has recently drawn the researchers' attention. Wang et al. studied the photocatalytic performance of ZnO/SnO_2 photocatalysts for Methyl Orange (MO) degradation [24]. They found that the photocatalytic activities of their samples reached the maximum value in case the Sn content and calcination temperature were about 33.3 mol% and 500°C, respectively. Subramanian et al. synthesized CRGO and $CRGO/SnO_2$ nanocomposite for photocatalytic degradation of methylene green dye [25]. According to their obtained results, SnO_2-C/annuum Reduced Graphene Oxide (CRGO) nanocomposite exhibited a photodegradation efficiency rate of 97.4%.

The results showed that Graphene-based semiconductor photocatalysts were well established for dye degradation applications in polluted water [25]. In this respect, the present study aimed to synthesize SnO_2/GO thin films with different concentrations of GO (0, 1, 2, 3, and 4 g/ml) using spin coating method where all the reaction parameters were carefully optimized to retain the good crystalline structure of samples. To this end, the structural, morphological, chemical, and optical properties as well as photocatalytic degradation of MO under UV light irradiation of SnO_2-pure and SnO_2/GO thin films were carefully studied.

2. Experimental section

2.1. Preparation of SnO_2 thin layer

One gram of Tin Chloride was mixed with five cc of ethanol and stirred for 15 min. The solution was covered to rest for 24 hours under stirring. The glass substrates were rinsed using ultrasonic bath for 30 min at 60°C and then, they were placed in the acetone for 5 min and dried. The resulting solution was spin coated on the layers at a speed of 5000 rpm for 1 minute, and this process was repeated 50 times. The prepared layers were preheated for 20 min at 200°C and calcined for three hours at 500°C.

2.2. Preparation of Graphene Oxide (GO) thin layer

GO sheets were prepared from graphite using the Hummers method, as previously reported by researchers [26]. To prepare GO solution, 10 g, 20 g, 30 g, and 40 g of GO were solved in 10 cc of ethanol and dispersed in ultrasonic for 10 min. The GO solution was spin coated on SnO_2 layers at a speed of 5000 rpm for one min, and this process was repeated 25 times. To dry the layers, they were placed at 40–50°C for 30 min. These samples containing different concentrations of GO (0, 1, 2, 3, and 4 g/ml) were called SnO_2-pure, SnO_2/GO-10, SnO_2/GO-20, SnO_2/GO-30, SnO_2/GO-40, respectively. Then, characterization was performed on the samples.

3. Sample characterization

Through X-Ray Diffraction (XRD) method, the crystal structures of the prepared thin films were characterized by a D8 Advance Bruker YT diffractometer via Cu-Kα radiation in the range of 10°–80°. The morphology of the layers was investigated using Field Emission Scanning Electron Microscopy (FESEM) performed on MIRA3 TESCAN-XMU microscope. X-Ray microanalysis system was supported by a Nano Trace LN-Cooled Si (Li) detector for Energy-Dispersive X-ray spectroscopy (EDX) analysis. Optical properties such as absorption and transmission spectra of the samples were studied using Ultraviolet-Visible (UV-Vis) device U3500 model. Room temperature Raman spectra were measured using micro-laser Raman spectrometer (Takram P50C0R10) in backscattering configuration, employing the 532 nm line of Nd:YAG laser as the excitation source.

4. Result and discussion

4.1. Structural properties

The crystalline structures of SnO_2-pure, SnO_2/GO-10, SnO_2/GO-20, SnO_2/GO-30, and SnO_2/GO-40 thin films with different concentrations of GO were recorded by XRD in the range of $2\theta = 10 - 80°$ using Cu-Kα radiation, the results of which are reported in Figure 1. Figure 1(a) shows the pure sample which confirms the formation of a crystalline structure without any additional peaks. In addition, SnO_2 peaks are located at $2\theta = 26.5, 33.8, 37.9$, and 51.7°, which correspond to (110), (101), (200), and (211) reflecting planes, respectively. According to the JCPDS (41–1445) card number, the pure sample is characterized by the cassiterite phase [27]. Figure 1(b)–(e) show the SnO_2-GO samples with different GO concentrations. According to these figures, compared to SnO_2 peaks, the GO peak intensity at an angle of 10° is quite high, thus confirming the presence of GO in samples. The

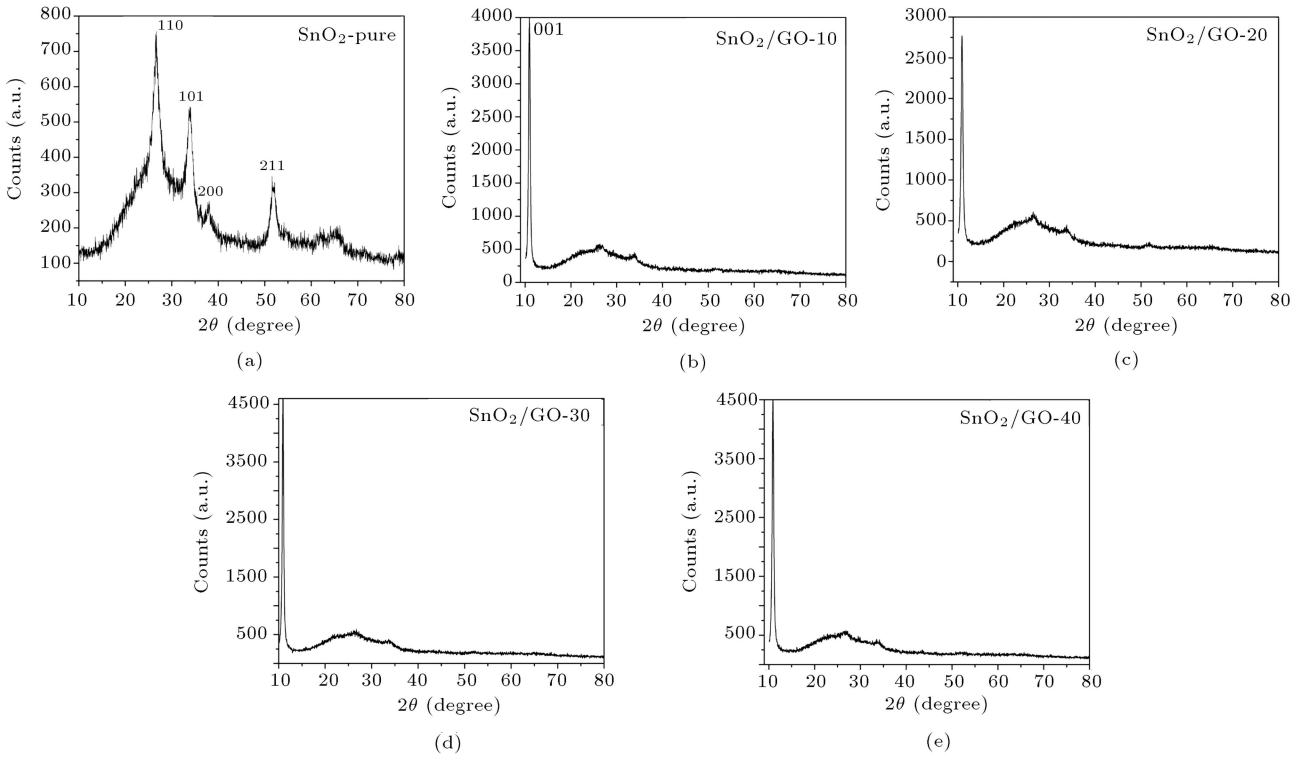

Figure 1. X-Ray Diffraction (XRD) patterns of (a) SnO_2-pure, (b) SnO_2/GO-10, (c) SnO_2/GO-20, (d) SnO_2/GO-30, and (e) SnO_2/GO-40 thin films.

peaks are quite sharp with high intensity, indicating good crystallinity of the GO structure. No additional peaks are observed in these figures. According to Scherrer equation, the average grain sizes of pure SnO_2, SnO_2/GO-10, SnO_2/GO-20, SnO_2/GO-30, and SnO_2/GO-40 thin films are 57, 70, 67, 65, and 60 nm, respectively, all in the nanometer range, resulting in significant dispersion across the grain boundaries. Hence, its mobility is low and we expect the resistivity of the layers to be high. The lattice parameter values of SnO_2-pure thin film are $a = 4.722$ Å, $b = 5.753$ Å, and $c = 5.245$ Å, respectively, all in good agreement with the results reported by other researchers [28,29].

4.2. Morphological analysis using FESEM, cross-sectional, and EDX

Microstructure and surface morphology of SnO_2-pure, SnO_2/GO-10, and SnO_2/GO-40 thin layers were characterized by FESEM images. FESEM results of these samples are shown in Figure 2. Figure 2(a) shows a

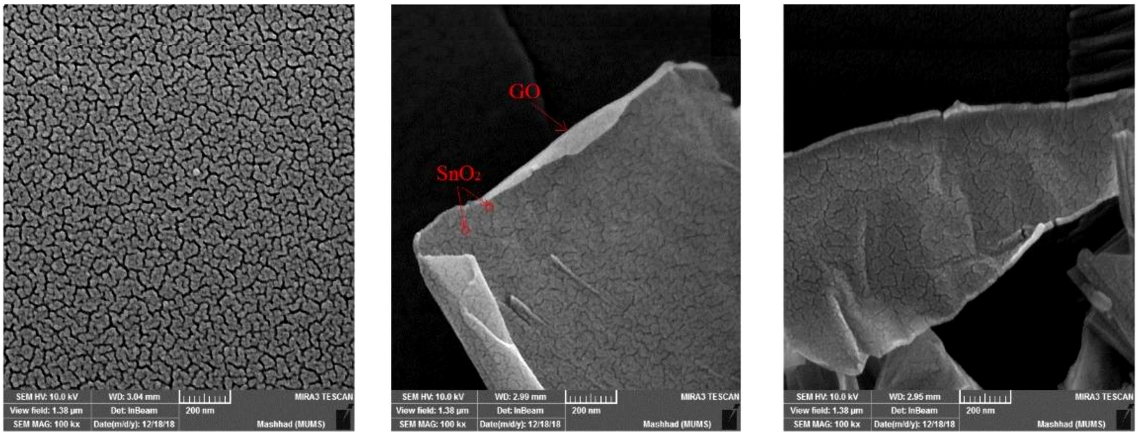

(a) SnO_2-pure (b) SnO_2/GO-10 (c) SnO_2/GO-40

Figure 2. Field Emission Scanning Electron Microscopy (FESEM) images of (a) SnO_2-pure, (b) SnO_2/GO-10, and (c) SnO_2/GO-40 thin films.

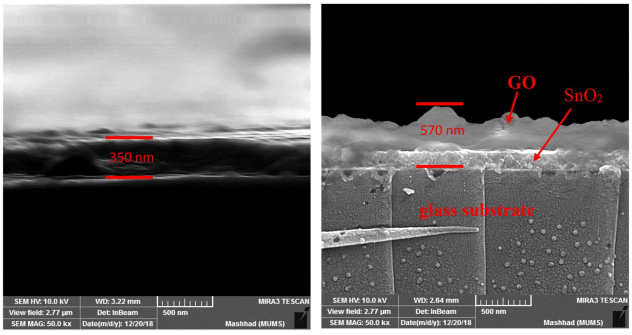

SnO_2-pure SnO_2/GO-40

Figure 3. Cross-section of (a) SnO_2-pure and (b) SnO_2/GO-40 thin films.

SnO_2-pure sample whose surface is completely uniform and smooth with a quite small size of grains, i.e., less than 100 nm. In SnO_2/GO-10 and SnO_2/GO-40 samples (Figure 2(b) and (c)), the GO plates are clearly shown to be overlapping together and covering the SnO_2 surface. The cross-sectional images of SnO_2-pure and SnO_2/GO samples are shown in Figure 3. According to the pure sample, the surface of the sample is quite uniform (with a thickness of 350 nm); however, after adding GO, the layer surface becomes completely rough (with a thickness of 570 nm). Characterized by wrinkled structures, GO sheets overlap each other, as shown in Figure 2(b) and (c). Hence, upon adding GO, plates can increase the thickness and surface roughness of the layers. To determine the composition type of the synthesized layers, EDX analysis was employed. Figure 4 illustrates the obtained results for SnO_2-pure layers in the presence of GO with concentrations of 1 and 4 g/ml. While Figure 4(a) presents the Sn- and O-related peaks only, Figure 4(b) and (c) show the carbon-related peaks that confirm the presence of GO in these structures.

4.3. Chemical properties: Raman spectroscopy

Raman spectroscopy is a non-destructive technique that is employed to obtain structural information about samples, especially about carbon structures. Figure 5 demonstrates the Raman spectra of SnO_2-pure, SnO_2/GO-10, and SnO_2/GO-40 thin films with different GO concentrations prepared by spin coating method. The main characteristic of the samples

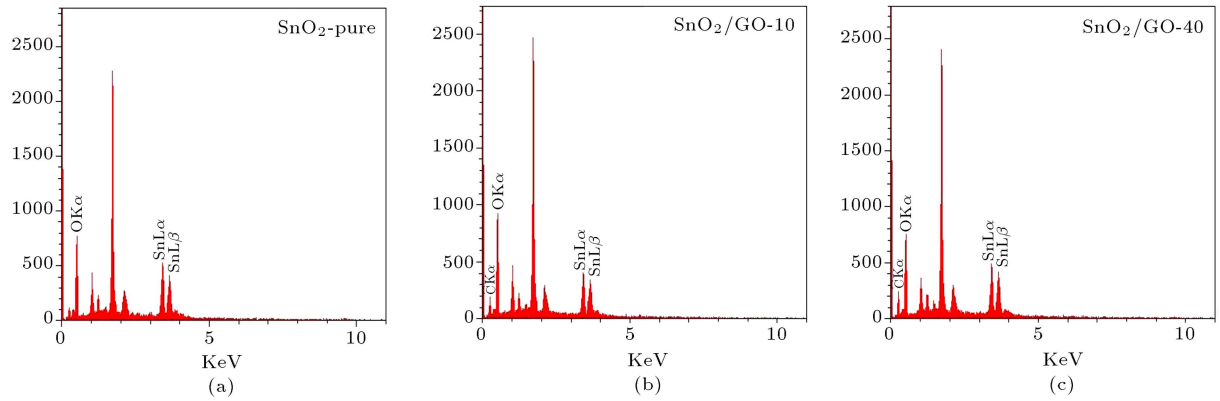

Figure 4. Energy Dispersive X-ray spectroscopy (EDX) analysis of (a) SnO_2-pure, (b) SnO_2/G-10, and (c) SnO_2/G-40 thin films.

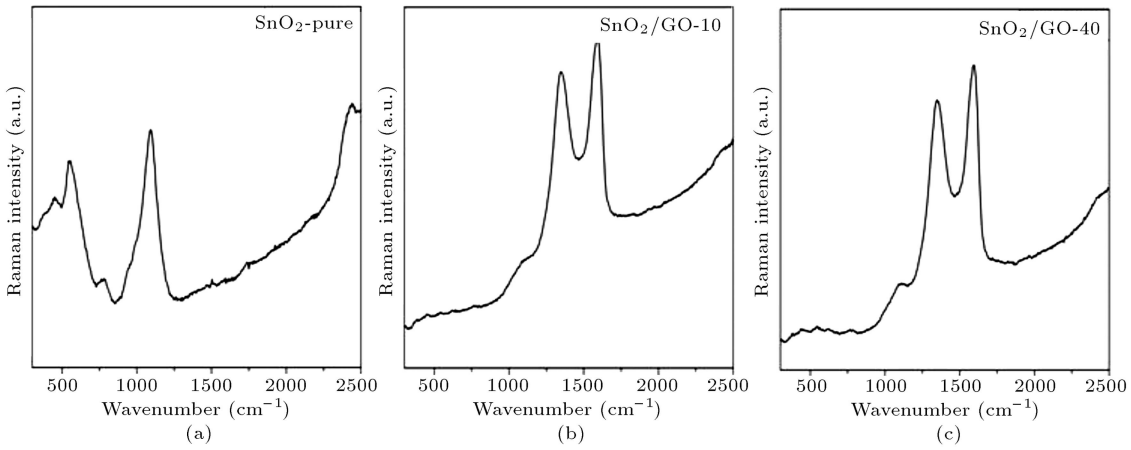

Figure 5. Raman spectra of (a) SnO_2-pure, (b) SnO_2/GO-10, and (c) SnO_2/GO-40 thin films.

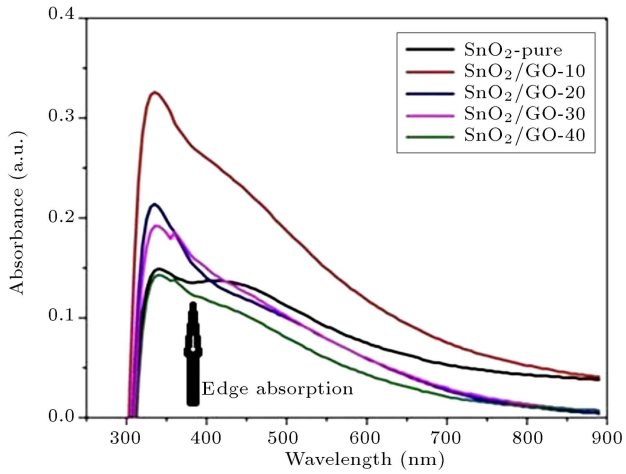

Figure 6. Ultraviolet-Visible (UV-Vis) spectrum of SnO_2-pure, SnO_2/GO-10, SnO_2/GO-20, SnO_2/GO-30, and SnO_2/GO-40 thin films with different Graphene Oxide (GO) concentrations.

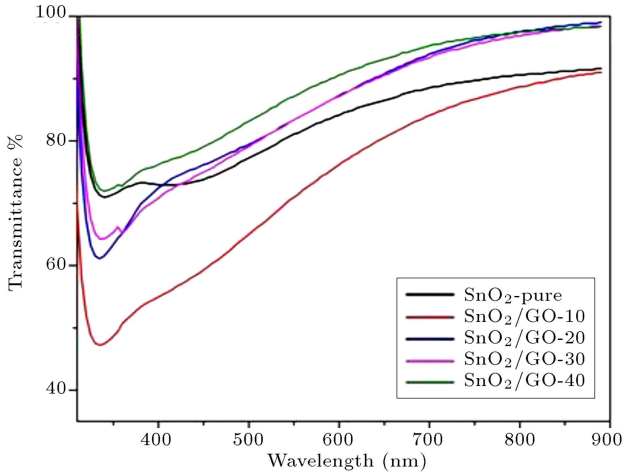

Figure 7. The transmittance spectra of SnO_2-pure, SnO_2/GO-10, SnO_2/GO-20, SnO_2/GO-30, and SnO_2/GO-40 thin films with different Graphene Oxide (GO) concentrations.

containing carbon in their structure is the presence of the G and D peaks that are indicative of the sp^2 carbon fluctuations arranged at the wavelengths of about 1580 cm^{-1} and 1350 cm^{-1}, respectively. Generally, the intensity of D peak is used to determine the disorder degree of the structure. According to the picture, the intensity of D peak is higher than that of G peak. Hence, the structure is very disorderly [30,31].

4.4. Optical properties

To confirm the capabilities of the optical properties of SnO_2-pure, SnO_2/GO-10, SnO_2/GO-20, SnO_2/GO-30, and SnO_2/GO-40 thin films with different GO concentrations, UV-Vis absorption spectroscopy was employed. UV-Vis absorption spectra of SnO_2/GO thin films were measured at a wavelength ranging from 250 to 900 nm. Figure 6 presents the UV-Vis absorption spectra of the synthesized thin films. The edge absorption for SnO_2/GO thin films was detected at 380 nm. For GO, red shift occurred in the range of 310 nm to 370 nm after the reduction of GO to rGO. A peak was observed with maximum absorption at 310 nm and the other neighboring high absorption peaks were also seen for SnO_2/GO thin films with different concentrations and a noticeable red shift in maximum absorption. This red shift occurred mainly due to the presence of semiconductor SnO_2 nanoparticles on the graphene sheet. Interestingly, in the case of SnO_2/G nanocomposites, the peak observed at 310 nm was associated with the graphene red-shifts at 340 nm, indicating an increase in the π-electron concentration followed by the reduction of sp^3 GO to sp^2-hybridization of carbon atoms [32]. The absorption edge red shift was observed at the higher energy band > 3.0 eV. The red shift in the band gap was observed due to the improved crystallinity of the thin film. The optical band gap of the film decreases with an increase in the grain size. The barrier height of the grain boundary increased with an increase in the grain size, thus resulting in a decrease in the band gap of the thin film. Through this test, it was found that the samples had good absorption in the visible light or UV range.

The spectral distributions of transmittance of SnO_2-pure, SnO_2/GO-10, SnO_2/GO-20, SnO_2/GO-30, and SnO_2/GO-40 thin films with different GO concentrations were evaluated with normal occurrence in the wavelength range of 250-900 nm, the results of which are shown in Figure 7. According to this figure, SnO_2-pure thin films exhibit high transmittance ranging from 70% to 90%. In the case of adding 10, 20, 30 g of GO, the transmittance would decrease. Further, upon increasing the concentration of GO up to 40, its transmittance would increase more than that of the pure sample. This finding may be attributed to the decrease in the grain size of these films, as was demonstrated by the calculations of the Scherrer relation in the XRD section with the increasing concentrations of GO.

From the transmittance spectra, the optical band gap energy of SnO_2/GO thin films can be calculated using Tauc's relation [33,34]:

$$(\alpha h\upsilon)^{1/n} = A(h\upsilon - E_g), \tag{1}$$

where $h\upsilon$ is the photon energy, α the absorption coefficient, A the constant, and E_g the band gap of the material. The exponent n depends on the type of the transition: for direct and allowed transition, $n = 1/2$; for indirect transition, $n = 2$; and for direct un-allowed transition, $n = 3/2$.

In order to calculate the direct band gap value, $(\alpha h\upsilon)^2$ versus $h\upsilon$ was plotted, as shown in Figure 8. The band gap value can be measured using the straight portion of the graph on $h\upsilon$ axis at $\alpha = 0$.

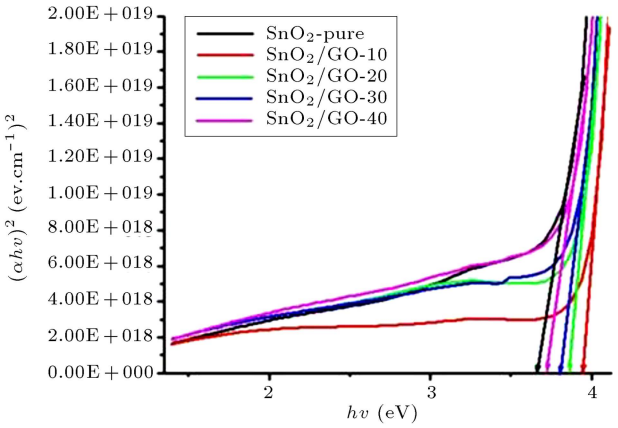

Figure 8. $(\alpha hv)^2$ versus hv for SnO_2-pure, SnO_2/GO-10, SnO_2/GO-20, SnO_2/GO-30, and SnO_2/GO-40 thin films with different Graphene Oxide (GO) concentrations.

The band gap value for SnO_2-pure is 3.56 eV, and the values for SnO_2/GO-10, SnO_2/GO-20, SnO_2/GO-30, and SnO_2/GO-40 are 3.65 eV, 3.7 eV, 3.8 eV and 3.9 eV, respectively. The band gap value for the thin films increased upon increasing the GO concentration, mainly due to decrease in the GO grain size resulting from nano-scale electron confinement, called "quantum size effect". In other words, electron is confined which in turn occupies less space than bulk; therefore, Valence Band Maximum (VBM) and Conduction Band Minimum (CBM) potentials are shifted more to + eV and − eV, respectively, causing a wider band gap. These results are in agreement with those reported in other studies [35]. The band gap of pure SnO_2 thin film was reported to be 3.42 eV in the study of Camacho-López et al., which increased up to 3.69 eV upon increasing the substrate temperature from 50 to 250°C [36]. Moreover, Soumia and Nasr-Eddine calculated the band gap of SnO_2 thin film as 3.6eV [37].

4.5. Photocatalytic activity

Under UV light irradiation, the photocatalytic activity of synthesized samples was measured using MO dye as the typical organic pollutant in water. Figure 9(a)–(c) demonstrate the UV-Vis absorption spectra of SnO_2-pure, SnO_2/GO-20, and SnO_2/GO-40 thin films with adsorbed MO in 60 min. First, 30 cc of 10 ppm of MO solution was put in a dark environment for 30 min to reach the absorption-desorption balance (sample A_0). The solutions were then irradiated by two UVC (200–280 nm) and UVB (280–315 nm) lamps of 18 W for 60 min (sample A_t). The percentage of MO degradation with absorption measurement in the wavelength of 464 nm was calculated through the following equation:

$$\frac{A_0 - A_t}{A_0} \times 100. \tag{2}$$

SnO_2-pure thin film did not exhibit the degradation efficiency under UV light irradiation for the 60 min time duration (Figure 9(a)). The degradation efficiency of SnO_2/GO-20 and SnO_2/GO-40 thin films was 2.2 and 3.4%, respectively. By adding GO concentration, the photocatalytic activity of the SnO_2 thin film increased. The presence of GO plates provided extra trapping sites for incoming photo-generated charge carriers, which resulted in better photocatalytic activity [38]. Karimabad et al. [39] investigated the photocatalytic activity of SnO_2 nanoparticles in the presence of MO. Their results indicated that as the time increased, the peak intensity decreased and it would disappear completely after 60 min (about 80–90% degradation). By comparing our results with those of Soumia and Nasr-Eddine [37], it seems that SnO_2 nanopowder has better photocatalytic properties than its thin film. Given the active surface area of the thin films was smaller than the nanopowder, the decomposition rate was much lower and the photocatalytic property of thin films was less than nanopowder. Similar results were also reported by researchers for other materials such as TiO_2 [40].

5. Conclusion

In this study, SnO_2-pure, SnO_2/GO-10, SnO_2/GO-20, SnO_2/GO-30, and SnO_2/GO-40 thin films with different Graphene Oxide (GO) concentrations were synthesized using spin coating method. The structural,

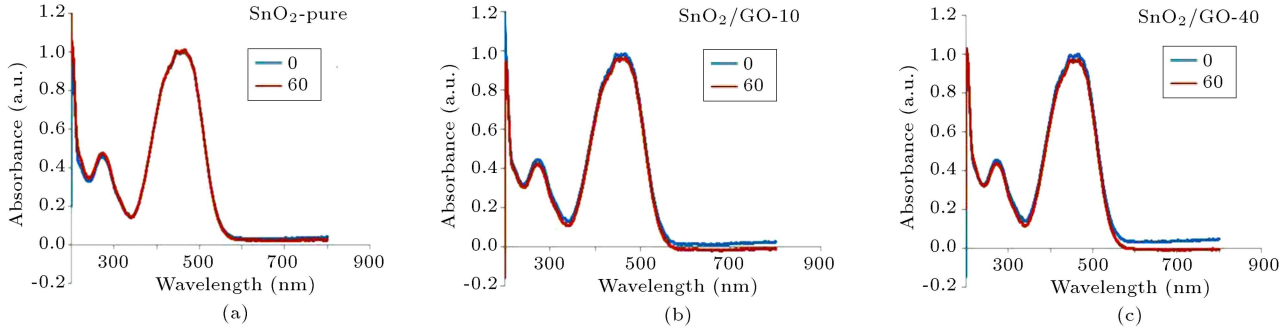

Figure 9. Typical Ultraviolet-Visible (UV-Vis) absorption spectra of Methyl Orange (MO) solutions after 60 min of UV irradiation in the presence of (a) SnO_2-pure, (b) SnO_2/GO-20, and (c) SnO_2/GO-40.

morphological, chemical, optical, and photocatalytic degradations of Methyl Orange (MO) under UV light irradiation were also studied. The X-Ray Diffraction (XRD) results showed that the peaks were quite sharp with very high intensity, indicating the good crystallinity of the GO structure. No additional peaks were observed. Field Emission Scanning Electron Microscopy (FESEM) images revealed that the surface of the pure sample was completely uniform and smooth and the size of the grains was very small, i.e., less than 100 nm. In SnO_2/GO samples, the GO plates clearly overlapped together and covered the surface of SnO_2. G and D peaks were indicative of the presence of GO arranged at the wavelengths of about 1580 cm^{-1} and 1350 cm^{-1}, respectively. The band gap value of SnO_2-pure was 3.56 eV which increased by increasing the GO concentration. The band gap value of the thin films also increased followed by an increase in the GO concentration. An increase in the band gap value led to an increase in the concentration that in turn resulted from a decrease in the particle size. Under UV light irradiation, the photocatalytic activity of the synthesized samples was measured using MO dye. Degradation efficiencies of SnO_2/GO-20 and SnO_2/GO-40 thin films were measured as 2.2 and 3.4%, respectively. The MO adsorption was completed on the surfaces of both GO and metal oxides using the prepared thin films.

References

1. Paul, E., Andreas, K., Russell, G.E., et al. "Band structure of indium oxide: Indirect versus direct band gap", *Phys. Rev, B.*, **75**(15), pp. 153205-1–153205-4 (2007).
2. Geeta, S., Raj, R., and Abhai, M. "Band-gap narrowing and band structure in degenerate tin oxide (SnO_2) films", *Phys. Rev. B.*, **44**(11), pp. 5672– 5680 (1991).
3. Jefferson, P.H., Hatfield, S.A., Veal, T.D., King, P.D.C., and McConville, C.F. "Bandgap and effective mass of epitaxial cadmium oxide", *Appl. Phys. Lett.*, **92**(2), pp. 022101–022103 (2008).
4. Leila, M., Boshra, G.S., and Abrishami, M. "Effects of Mn doping on electrical properties of ZnO thin films", *Modern Physics Letters B.*, **30**(4), pp. 1650024–1650028 (2016).
5. Andreas, E. and Wilfried, L. "Solution-deposited PEDOT for transparent conductive applications", *MRS Bulletin*, **36**(10), pp. 794–798 (2011).
6. Kazuhiro, N. and Kohtaro, T. "Production of transparent conductive films with inserted SiO_2 anchor layer, and application to a resistive touch panel", *Electronics and Communications in Japan*, **84**(7), pp. 39–44 (2001).
7. Maciej, S., Katarzyna, Z., Sylwia, W., et al. "Comparison of ZnO: Al, ITO and carbon nanotube transparent conductive layers in flexible solar cells applications", *Materials Science and Engineering: B.*, **177**(15), pp. 1292–1298 (2012).
8. Lee-May, H., Chih-Wei, H., Han-Chang, L., et al. "Photovoltaic electrochromic device for solar cell module and self-powered smart glass applications", *Solar Energy Materials and Solar Cells*, **99**, pp. 154–159 (2012).
9. Maciej, S., Katarzyna, Z., Mirosław, S., and Michał, G. "AZO layers deposited by PLD method as flexible transparent emitter electrodes for solar cells", *Microelectronic Engineering*, **127**, pp. 57–60 (2014).
10. Qiu, Y., Hermawan, H., Gordon, I., and Poortmans, J. "Direct current sputtered aluminum-doped zinc oxide films for thin crystalline silicon heterojunction solar cell", *Materials Chemistry and Physics*, **141**(2), pp. 744–751 (2013).
11. Beck, A., Bednorz, J.G., Gerber, Ch., Rossel, C., and Widmer, D. "Reproducible switching effect in thin oxide films for memory applications", *Appl. Phys. Lett.*, **77**(1), pp. 139–141 (2000).
12. Radhouane, B.H.T., Takayuki, B., Yutaka, O., et al. "Tin doped indium oxide thin films: Electrical properties", *Journal of Applied Physics*, **83**(5), pp. 2631–2645 (1998).
13. Kim, H. and Gilmore, C.M. "Electrical, optical, and structural properties of indium-tin-oxide thin films for organic light-emitting devices", *Journal of Applied Physics*, **86**(11), pp. 6451–6461 (1999).
14. Kim, H., Piqué, A., Horwitz, J.S., Mattoussi, H., et al. "Indium tin oxide thin films for organic light-emitting devices", *Appl. Phys. Lett.*, **74**(23), pp. 3444–3446 (1999).
15. Tadatsugu, M. "Substitution of transparent conducting oxide thin films for indium tin oxide transparent electrode applications", *Thin Solid Films*, **516**(7), pp. 1314–1321 (2008).
16. Kim, H.J. Horwitz, S., Kushto, G., et al. "Effect of film thickness on the properties of indium tin oxide thin films", *Journal of Applied Physics*, **88**(10), pp. 6021–6025 (2000).
17. Peelaers, H., Kioupakis, E., and Van de Walle, C.G. "Fundamental limits on optical transparency of transparent conducting oxides: Free-carrier absorption in SnO_2", *Appl. Phys. Lett.*, **100**(1), pp. 011914–011917 (2012).
18. Dattoli, E.N., Wan, Q., Guo, W., Chen, Y., Pan, X., and Lu, W. "Fully transparent thin-film transistor devices based on SnO_2 nanowires", *Nano Lett*, **7**(9), pp. 2463–2469 (2007).
19. Bagheri-Mohagheghi, M.M. and Shokooh-Saremi, M. "The influence of Al doping on the electrical, optical

and structural properties of SnO_2 transparent conducting films deposited by the spray pyrolysis technique", *J. Phys. D: Appl. Phys.*, **37**(8), pp. 1248–1253 (2004).

20. Ogale, S.B., Choudhary, R.J., Buban, J.P., et al. "High temperature ferromagnetism with a giant magnetic moment in transparent co-doped SnO(2-delta)", *J. Phys Rev Lett.*, **91**(7), pp. 0772052–0772059 (2003).

21. Philip, J., Punnoose, A., Kim, B.I., et al. "Carrier-controlled ferromagnetism in transparent oxide semiconductors", *Nature Materials*, **5**(4), pp. 298–304 (2006).

22. HarinathBabu, S., Kaleemulla, S.N., Madhusudhana, R., and Krishnamoorthi, C. "Indium oxide: A transparent, conducting ferromagnetic semiconductor for spintronic applications", *Journal of Magnetism and Magnetic Materials*, **416**(33), pp. 66–74 (2016).

23. Anshu, S., Achary, S.N., Manjanna, J., Jayakumar, O., et al. "Colloidal Fe-doped indium oxide nanoparticles: Facile synthesis, structural, and magnetic properties", *J. Phys. Chem. C.*, **113**(9), pp. 3600–3606 (2009).

24. Wang, C., Wang, X., Xu, B.Q., Zhao, J., Mai, B., Peng, P., Sheng, G., and Fu, J. "Enhanced photocatalytic performance of nanosized coupled ZnO/SnO_2 photocatalysts for methyl orange degradation", *Journal of Photochemistry and Photobiology A: Chemistry*, **168**(1), pp. 47–52 (2004).

25. Ramanathan, S., Radhika, N., Padmanabhan, D., Durairaj, A., Selvin, S.P., Lydia, S., Kavitha, S., and Vasanthkumar, S. "Eco-friendly synthesis of CRGO and $CRGO/SnO_2$ nanocomposite for photocatalytic degradation of methylene green dye", *ACS Omega* **5**, pp. 158–169 (2020).

26. Leila, S. and Anjali, A. "Graphene oxide synthesized by using modified hummers approach", *International Journal of Renewable Energy and Environmental Engineering*, **02**(1), pp. 58–63 (2014).

27. Zhang, M., Lei, D., Du, Z., Yin, X., Chen, L., Li, Q., Wang, Y., and Wang, T. "Fast synthesis of SnO_2/graphene composites by reducing graphene oxide with stannous ions", *J. Mater. Chem.*, **21**(6), pp. 1673–1676 (2011).

28. Suito, K., Kawai, N., and Masuda, Y. "High pressure synthesis of orthorhombic SnO_2", *Materials Research Bulletin*, **10**(7), pp. 677–680 (1975).

29. Mahesh, B., Pallavi, S., and Veda, R. "Synthesis of nanocrystalline SnO_2 powder by amorphous citrate route", *Materials Letters*, **57**(9–10), pp. 1604–1611 (2003).

30. Shohany, B.G. and Zak, A.K. "Doped ZnO nanostructures with selected elements - Structural, morphology and optical properties: A review," *Ceramics International*, **46**(5), pp. 5507–7000 (2020).

31. Yoo, D.T., Cuong, V., and Pham, V. "Enhanced photocatalytic activity of graphene oxide decorated on TiO_2 films under UV and visible irradiation", *Current Applied Physics*, **11**(3), pp. 805–808 (2011).

32. Wang, W., Kapitanova, O., Ilanchezhiyan, P., et al. "Self-assembled MoS_2/rGO nanocomposites with tunable UV-IR absorption", *RSC Adv.*, **49**(8), pp. 2410–2417 (2018).

33. Saleem, A., Ullah, N., Khursheed, K., et al. "Graphene oxide–TiO2 nanocomposite films for electron transport applications", *Journal of electronic materials*, **47**(7), pp. 3749–3756 (2018).

34. Mahmood, H., Habib, A., Mujahid, M., Tanveer, M., Javed, S., and Jamil, A. "Band gap reduction of titania thin films using graphene nano-sheets", *Materials Sciencein Semiconductor Processing*, **24**(1) pp. 193–199 (2014).

35. Razeghizadeh, A.R., Zalaghi, L., Kazeminezhad, I., Rafee, V. "Growth and optical properties investigation of pure and al-doped SnO_2 nanostructures by sol-gel method", *Iran. J. Chem. Chem. Eng.*, **36**(5) pp. 1–8 (2017).

36. Camacho-López M.A., Galeana-Camacho J.R., Esparza-Garcá, A., et al. "Characterization of nanostructured SnO_2 films deposited by reactive DC-magnetron sputtering", *Superficies y Vacío*, **26**(3) pp. 95–99 (2013).

37. Soumia, B. and Nasr-Eddine, H. "Concentration influence on structural and optical properties of SnO_2 thin films synthesized by the spin coating technique", *Journal of Physics: Conference Series*, **758**(1), p. 012007 (2016).

38. Syed Irfan, L. Fu, L., et al. "Effect of graphene oxide nano-sheets on structural, morphological and photocatalytic activity of BiFeO3-based nanostructures", *Nanomaterials (Basel)*, **9**(2) p. 1337 (2019).

39. Karimabad, A.E.B., Ghanbari, D., Salavati-Niasari, M., and Nejati-Moghadam, L. "Photo-catalyst tin dioxide: synthesis and characterization different morphologies of SnO_2 nanostructures and nanocomposites", *J Mater Sci: Mater Electron*, **29**, pp. 1238–1245 (2015).

40. Damian, W., Michal, M., Michalina, K., et al. "Influence of Nd-doping on photocatalytic properties of TiO2 nanoparticles and thin film coatings", *International Journal of Photoenergy*, **18**(51) pp. 29928–29942 (2014).

Biographies

Ali Hussain Abdalrazzaq Jalaukhan was born in Kerbala, Iraq in 1962. He received his BSc in Physics in 1983 from university of Mosul, Iraq. He received his MSc degree in Solid State Physics from Baghdad University, Iraq in 1991. The title of his MSc dissertation was "The Optical and Electrical Properties of Thin Films Compound $CuInSe_2$". The title of his PhD thesis was "Microstructure and Optoelectronics Characterizations of Ga_xSb_{1-x}/GaAs Heterojunction", which

was completed in 2012. Later, he joined University of Kerbala as a teacher and researcher. His current research interests include thin films, characterization of carbon nanostructures, graphene nano plates, antibacterial studies, and self-cleaning applications. He has published research papers in many conferences and journals.

Boshra Ghanbari Shohany was born in Iran in 1981. She received her BSc in Physics and her MSc in Solid State Physics from Ferdowsi University of Mashhad, Iran in 2004 and 2010, respectively. Her PhD thesis title was "Band gap modification of Graphdiyne nanoribbons and nanotubes for: manufacturing a dopant-free mono-material transistor by numerical computational method" which was defended at Ferdowsi University and completed in 2016. Then, she joined the Borhan Nanoscale Company, Mashhad, Iran as a managing director and researcher. Her current research focuses on the synthesis and characterization of carbon nanostructures and metal oxides for photocatalytic dye degradation, antibacterial studies, and self-cleaning applications. Shohany has published 12 research papers in international journals.

Reihane Etefagh was born in Iran in 1984. She received her BSc in Physics and her MSc in Solid State Physics from Azad university of Mashhad, Iran in 2007 and 2015, respectively. Her PhD thesis title was "Synthesis and characterization of structural and electrochemical properties and investigation the doping effect of aluminum and indium on cathode nanostructures Li(Li-Mn-Ni-Co)O_2 for using in lithium-ion batteries" at Guilan University, which was completed in 2018. Then, she joined the Borhan Nanoscale Company, Mashhad, Iran as a researcher. Her current research focuses on the synthesis and characterization of carbon nanostructures and metal oxides for photocatalytic dye degradation, antibacterial studies, and self-cleaning applications.